3380 *Chem. Mater.* **2009,** *21,* 3380–3390
DOI:10.1021/cm901140u

CHEMISTRY OF MATERIALS
Article

Negative Thermal Expansion in the Aluminum and Gallium Phosphate Zeotypes with CHA and AEI Structure types

Mahrez Amri and Richard I. Walton*

Department of Chemistry, University of Warwick, Coventry, CV4 7AL, United Kingdom

Received April 24, 2009. Revised Manuscript Received June 8, 2009

We present a high-resolution powder X-ray diffraction study as a function of temperature of three structurally related, open-framework phosphates: $AlPO_4$ and $GaPO_4$ with the CHA-type structure (AlPO-34 and GaPO-34, respectively) and $AlPO_4$ with the AEI-type framework (AlPO-18). On the basis of refined lattice parameters (in space group $R\bar{3}$ for the CHA materials and *Cmcm* for AEI) all three materials show negative thermal expansion. In the case of AlPO-34, this is found from 110 to 450 K; for GaPO-34, the volume expansion is net negative above 210 K, below which there is a phase transition to a new monoclinic polymorph. For AlPO-18, the behavior of the negative thermal expansion (110−450 K) can be related directly to AlPO-34 by using polar plots in certain specific crystallographic planes that imply that certain common structural features are responsible for the behavior. We compare the results with published data for SiO_2 with the CHA-type structure; this shows that the isoelectronic $AlPO_4$ has rather similar thermal behavior but that preparation of the $GaPO_4$ homologue provides a way of tuning the magnitude and anisotropy of thermal expansivity. Rietveld refinement of atomic structure as a function of temperature for each material reveals that structural units common to each (double six-rings and eight-ring windows) behave similarly for each material as a function of temperature.

1. Introduction

Interest in the phenomenon of negative thermal expansion, i.e. concerning materials that show a counterintuitive contraction upon heating, is not just a scientific curiosity, because there are in fact many technological applications of the property in areas ranging from engineering to nanotechnology.[1−3] This includes uses as additives in composites to yield low (or zero) thermal expansion materials for precision optical and electronic applications or more generally as low thermal shock ceramics. Negative thermal expansion has now been reported in several distinct families of inorganic solids. This includes the mixed-oxide materials ZrW_2O_8,[4] $Sc_2(WO_4)_3$,[5] each with various compositional analogues;[6] a number of open-framework silicates and phosphates;[7] pyrophosphates MP_2O_7,[8] some of which show negative thermal expansion at high temperature; alloys;[9,10] nitrides;[11] metal organic framework materials;[12] and recently metal cyanide networks, where thermal expansion coefficients of unprecedented magnitude ("colossal") have been reported.[13] For many of these materials, the idea of rigid unit modes, with a specific structural flexibility, such as M−O−M′ or M−CN−M′ linkages, is often used to explain how negative thermal expansion results despite the expected positive thermal expansion of individual chemical bonds, since transverse vibrational modes of the linking atom may result in a shortening of the M−M distances with temperature.[14,15] In other cases, more unusual mechanisms may be responsible such as magnetic or electronic transitions that give rise to rearrangements of valence electrons and shortening of chemical bonds with temperature.[10] Understanding the relationship between structural chemistry and the resulting physical property is clearly of the utmost importance to design new solids with controlled thermal expansivity and to tune the performance of existing materials.

*Author for correspondence. E-mail: r.i.walton@warwick.ac.uk.

(1) Evans, J. S. O. *J. Chem. Soc., Dalton Trans.* **1999**, 3317.
(2) Barrera, G. D.; Bruno, J. A. O.; Barron, T. H. K.; Allan, N. L. *J. Phys.: Condens. Matter* **2005**, *17*, R217–R252.
(3) Sleight, A. W. Negative Thermal Expansion. In Thermal Conductivity; Dinwiddie, R. B., White, M. A., McElroy, D. L., Eds.; DEStech: Lancaster, PA, 2006; Vol. *28*, pp 131−139.
(4) Mary, T. A.; Evans, J. S. O.; Vogt, T.; Sleight, A. W. *Science* **1996**, *272*, 90.
(5) Evans, J. S. O.; Mary, T. A.; Sleight, A. W. *J. Solid State Chem.* **1998**, *137*, 148.
(6) Evans, J. S. O.; Mary, T. A.; Sleight, A. W. *J. Solid State Chem.* **1997**, *133*, 580.
(7) Lightfoot, P.; Woodcock, D. A.; Maple, M. J.; Villaescusa, L. A.; Wright, P. A. *J. Mater. Chem.* **2001**, *11*, 212.
(8) White, K. M.; Lee, P. L.; Chupas, P. J.; Chapman, K. W.; Payzant, E. A.; Jupe, A. C.; Bassett, W. A.; Zha, C. S.; Wilkinson, A. P. *Chem. Mater.* **2008**, *20*, 3728.
(9) Hausch, G.; Bacher, R.; Hartmann, J. *Physica B* **1989**, *161*, 22.
(10) Salvador, J. R.; Gu, F.; Hogan, T.; Kanatzidis, M. G. *Nature* **2003**, *425*, 702.
(11) Takenaka, K.; Takagi, H. *Appl. Phys. Lett.* **2005**, *87*, 261902.
(12) Wu, Y.; Kobayashi, A.; Halder, G. J.; Peterson, V. K.; Chapman, K. W.; Lock, N.; Southon, P. D.; Kepert, C. J. *Angew. Chem., Int. Ed.* **2008**, *47*, 8929.
(13) Goodwin, A. L.; Calleja, M.; Conterio, M. J.; Dove, M. T.; Evans, J. S. O.; Keen, D. A.; Peters, L.; Tucker, M. G. *Science* **2008**, *319*, 794.
(14) Hammonds, K. D.; Heine, V.; Dove, M. T. *J. Phys. Chem. B* **1998**, *102*, 1759.
(15) Tao, J. Z.; Sleight, A. W. *J. Solid State Chem.* **2003**, *173*, 442.

Published on Web 06/29/2009

Zeolites are a well-known class of framework materials that were initially predicted to possess negative thermal expansivity on the basis of computer simulations, a fact verified first for Na-zeolite X (FAU-type) by Couves et al.[16] Subsequently a larger number of zeolites and zeotypes, i.e., structurally similar compositional variants such as aluminum phosphates (AlPOs), have been proven to show negative thermal expansion over large temperature ranges.[7] Noteworthy examples include AlPO-17 (ERI-type structure), which shows the largest negative volumetric thermal expansion coefficient of any oxide material ($\alpha_V = -35.1 \times 10^{-6}\ K^{-1}$)[17] and whose thermal behavior had also been predicted by computer simulation,[18] and siliceous faujasite (FAU-type), where a model involving the transverse vibrations of two-coordinate, bridging oxygens was proposed from Rietveld refinement of powder X-ray data.[19] In 2001, Lightfoot et al. suggested that negative thermal expansion was widespread in zeolites, although they noted that there were materials among the family where strong positive thermal expansion was actually seen.[7] Since then, a complex relationship between zeolite structure and thermal expansivity has emerged in which subtle changes in long-range structure can result in dramatic changes in thermal expansivity: for example at a monoclinic to orthorhombic phase transition (~360 K) in the siliceous material silicalite (MFI-type), the sign of the volume thermal expansion coefficient changes from positive to negative, but the temperature of this transition is very dependent on the presence of metal substituents and also hydroxyl content.[20−23] Similar behavior was seen in siliceous ferrierite (FER-type) by single crystal diffraction where a second-order transition from *Pnnm* to *Immm* symmetry gave a switch in the sign of the volume thermal expansivity, driven by transverse vibrations of Si−O−Si linkages at high temperature.[24] In the case of the siliceous zeolite with IFR structure type, the volume thermal expansivity is net negative but is highly anisotropic, being negative along two crystal axes and positive along the third and a variable temperature single-crystal X-ray diffraction study suggested that this anisotropy is related to the anisotropic crystal structure.[25]

Zeolites are attractive to study with regard to further understanding the structural origin of negative thermal expansion in extended structures, since there is now available a family of over 190 structure types, many of which can be prepared with a variety of chemical compositions.[26] It has been proposed that the open structures of zeolites coupled with flexible two-coordinate oxygen linkers between framework metals, is responsible for the common occurrence of negative thermal expansivity,[7] but there are actually few systematic structural studies focused on the underlying mechanism of the behavior. In particular, there are as yet relatively few studies of the atomic-scale structure of zeolites with temperature (in many cases, just the variation of the lattice parameters with temperature has been reported) and no studies that have focused on isostructural analogues of the same framework type in order to investigate the effect of the chemical composition on thermal behavior. This was the aim of the present work: we have selected three materials, two of which are phosphates with the CHA-type structure, and one a phosphate with the AEI-type structure, a closely related framework, Figure 1. Both structures are made up of double six rings, to yield an open net in which channels bounded by eight-rings are present: they may be thought of a stacking variants of the same secondary building units.

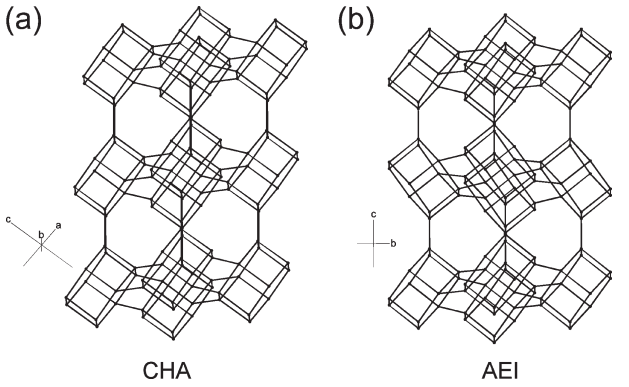

Figure 1. Relationship between (a) CHA-type and (b) AEI-type structures. Only T atoms and bonds between them are shown, using the convention for representing zeolite frameworks. Coordinates from the IZA structure database for these idealized structures.

The CHA-type structure is named after the mineral chabazite, an aluminosilicate that contains a variety of occluded alkali and alkali earth metal cations along with water in its natural form, and for which the thermal behavior above room temperature of a natural specimen has recently been reported (although it is complex because of the presence of the extra-framework species and water loss at certain temperatures).[27] The thermal behavior of SiO_2 with the CHA-type structure (which is free of any extra-framework species) has already been studied by two groups using diffraction methods, and negative thermal expansion was detected from 293 to 873 K. Woodcock et al. used Rietveld analysis of powder neutron diffraction to study CHA-SiO_2,[28]

(16) Couves, J. W.; Jones, R. H.; Parker, S. C.; Tschaufeser, P.; Catlow, C. R. A. *J. Phys.: Condens. Matter* **1993**, *5*, L329.
(17) Attfield, M. P.; Sleight, A. W. *Chem. Mater.* **1998**, *10*, 2013.
(18) Tschaufeser, P.; Parker, S. C. *J. Phys. Chem.* **1995**, *99*, 10609.
(19) Attfield, M. P.; Sleight, A. W. *Chem. Commun.* **1998**, 601.
(20) Park, S. H.; Kunstleve, R. W. G.; Graetsch, H.; Gies, H. *Stud. Surf. Sci. Catal.* **1997**, *105*, 1989.
(21) Marinkovic, B. A.; Jardim, P. M.; Saavedra, A.; Lau, L. Y.; Baehtz, C.; de Avillez, R. R.; Rizzo, F. *Microporous Mesoporous Mater.* **2004**, *71*, 117.
(22) Sen, S.; Wusirika, R. R.; Youngman, R. E. *Microporous Mesoporous Mater.* **2006**, *87*, 217.
(23) Marinkovic, B. A.; Jardim, P. M.; Rizzo, F.; Saavedra, A.; Lau, L. Y.; Suard, E. *Microporous Mesoporous Mater.* **2008**, *111*, 110.
(24) Bull, I.; Lightfoot, P.; Villaescusa, L. A.; Bull, L. M.; Gover, R. K. B.; Evans, J. S. O.; Morris, R. E. *J. Am. Chem. Soc.* **2003**, *125*, 4342.
(25) Villaescusa, L. A.; Lightfoot, P.; Teat, S. J.; Morris, R. E. *J. Am. Chem. Soc.* **2001**, *123*, 5453.
(26) http://www.iza-structure.org/databases/; International Zeolite Association, **2009**.
(27) Zema, M.; Tarantino, S. C.; Montagna, G. *Chem. Mater.* **2008**, *20*, 5876.
(28) Woodcock, D. A.; Lightfoot, P.; Villaescusa, L. A.; Diaz-Cabanas, M. J.; Camblor, M. A.; Engberg, D. *Chem. Mater.* **1999**, 2508.

whereas Martinez-Iñesta and Lobo used pair distribution function (PDF) analysis of high energy X-ray diffraction scattering data to study the material at two temperatures, 308 and 753 K.[29] As we will discuss further below, the magnitude of the linear thermal expansivity coefficients from these previous studies on seemingly the same material was different between the two studies. By comparing closely related phosphate analogues, we hope to gain a greater understanding of the origin of the negative thermal expansion property and how it might potentially be tuned by isomorphous substitution.

2. Experimental Section

2.1. Sample Preparation. Synthesis was based on published methods for AlPO-34 (using piperidine as template), AlPO-18 (tetraethylammonium hydroxide as template), and GaPO-34 (pyridine as template). AlPO-34 was synthesized following the protocol based on that of Tuel et al.[30] using a relative molar gel composition of Al_2O_3:P_2O_5:HF:2 piperidine:100 H_2O obtained by dispersing 1 g of aluminum isopropoxide (99.99 wt %, Aldrich) in 8.51 g of deionized water. Successive addition of 1.138 g of orthophosphoric acid (85 wt % in water, Fisher), 0.241 g of hydrofluoric acid (40 wt % in water, Fluka), and 0.833 g of piperidine (99%, Fluka) was then made to the suspension with vigorous stirring. The final gel was transferred to a Teflon-lined stainless steel autoclave (~50% fill) and heated at 190 °C for 4 days. The product of the reaction was recovered, washed with deionized water then filtered through coarse filter paper, and finally dried at 70 °C in air overnight. The structural analogue GaPO-34 was synthesized using pyridine as structure directing agent, as described by Schott Darie et al.[31] An amorphous gallium oxide source was prepared by heating gallium nitrate hydrate (Aldrich) at 250 °C for 24 h in air. The relative molar composition of the starting mixture was Ga_2O_3:P_2O_5:HF:70H_2O:1.7 pyridine. This was obtained by successive addition to 3.18 g of deionized water with vigorous stirring of 0.61 g of orthophosphoric acid (85 wt % in water, Fisher), 0.5 g of Ga_2O_3, 0.133 g of hydrofluoric acid (40 wt % in water, Fluka), and finally, 0.36 g of pyridine (Fisher, 99%) as structure directing agent. The final gel was stirred for 2 h at room temperature and then transferred to a Teflon-lined stainless steel autoclave (50% fill) for 24 h at 170 °C for crystallization. The final product was washed with distilled water and filtered through coarse filter paper and finally dried in air at 70 °C overnight. For AlPO-18, the synthesis procedure was based on that reported by Simmen et al.[32] The material was synthesized by dispersing 1 g of $Al_2O_3 \cdot 1.9\ H_2O$ (SASOL Ltd.) in 2.21 g of distilled water, and 1.61 g of orthophosphoric acid (85 wt % in water, Fisher) was then added to the previous suspension and mixed for 15 min for homogenization. A prepared mixture of 3.07 g of tetraethyl ammonium hydroxide (TEAOH) (35 wt % in water, Aldrich) and 0.24 g of hydrochloric acid (37 wt % in water, Fisher) was then added to the previous mixture. The final mixture was stirred for 2 h to obtain a white fluid gel with the relative molar composition of 0.33HCl:0.67$(TEA)_2O$:Al_2O_3:P_2O_5:35H_2O, which was transferred to a Teflon-lined stainless steel autoclaves (50% fill) for crystallization at 150 °C for 7 days. The product of the reaction was filtered through coarse filter paper, centrifuged, washed with distilled water, and dried at 180 °C for 2 h.

2.2. Laboratory Characterization. Laboratory powder XRD (Siemens D5000 with Cu Kα radiation) allowed sample identification and verified sample purity by comparison to simulated patterns from published structures. TGA (Perkin-Elmer Pyris Diamond TG/DTA apparatus with ~ 10 mg samples heated in platinum or alumina crucibles at 10 °C min^{-1}) indicated the temperatures need for template removal (see the Supporting Information). Calcination was then performed for AlPO-34 and AlPO-18 by heating at 700 and 600 °C in a tube furnace for 2 and 16 h, respectively. Powder XRD showed that the calcined materials hydrate rapidly in air (as shown previously for AlPO-34[30]) with a lowering of symmetry and broadening of Bragg peaks, but that on reheating above 200 °C for 2 h this water was removed to yield the calcined, dehydrated phase and the samples were then stable up to at least 800 °C; this was verified using an MRI TC-Basic heating stage on the powder diffractometer with the sample packed into an alumina sample holder. Therefore, the calcined samples of AlPO-34 and AlPO-18 were transferred to silica glass (1 mm diameter) capillaries and heated to 200 °C within each capillary before immediate sealing prior to high-resolution powder XRD experiments (see below). In the case of GaPO-34, the material proved to be unstable after calcination, collapsing after standing in air even after 30 min to yield an amorphous material, and so calcination was performed on a sample held within a 1 mm silica capillary for 450 °C for 1 h before immediate sealing while hot prior to measurement of high-resolution diffraction data. In the absence of moisture, the calcined, dehydrated sample of GaPO-34 then proved stable on repeated heating and cooling cycles.

2.3. Powder X-ray Diffraction. Data were recorded from the three materials contained within thin-walled silica glass capillaries on Beamline ID31 of the European Synchrotron Radiation Facility.[33] Samples were heated from ~100 to ~450 K in 50 K intervals using an Oxford Crysosystems 700 series nitrogen cryostream device. Temperature was measured accurately using a thermocouple situated close to the sample and calibrated using a Pt thermocouple.[34] The program Fullprof[35] was used to refine cell parameters using a Le Bail extraction of peak intensities with a pseudo-Voigt peak shape function to describe the profile,[36] with an additional correction for the asymmetry due to axial divergence for low-angle peaks,[37] and then to perform Rietveld analysis to yield refined crystal structures at each temperature. Details of the full structural analysis using the Rietveld method are described below for each material.

3. Results and Discussion

3.1. Thermal Expansivity. Unit-cell parameters of the two CHA-type materials AlPO-34 and GaPO-34 were determined by Le Bail extraction of peak intensities in the hexagonal setting of the trigonal space group $R\bar{3}$ (No. 148), consistent with a published structure of calcined,

(29) Martinez-Iñesta, M. M.; Lobo, R. F. *J. Phys. Chem.B* **2005**, *109*, 9389.
(30) Tuel, A.; Caldarelli, S.; Meden, A.; McCusker, L. B.; Baerlocher, C.; Ristic, A.; Rajic, N.; Mali, G.; Kaucic, V. *J. Phys. Chem. B* **2000**, *104*, 5697.
(31) Schott-Darie, C.; Kessler, H.; Soulard, M.; Gramlich, V.; Benazzi, E. *Stud. Surf. Sci. Catal.* **1994**, *84*, 101.
(32) Simmen, A.; McCusker, L. B.; Baerlocher, C.; Meier, W. M. *Zeolites* **1991**, *11*, 654.
(33) Fitch, A. N. *J. Res. Natl. Inst. Stand. Technol.* **2004**, *109*, 133.
(34) Margiolaki, I., Personal Communication **2008**.
(35) Rodriguez-Carvajal, J. *Physica B* **1993**, *192*, 55.
(36) Thompson, P.; Cox, D. E.; Hastings, J. B. *J. Appl. Crystallogr.* **1987**, *20*, 79.
(37) Finger, L. W.; Cox, D. E.; Jephcoat, A. P. *J. Appl. Crystallogr.* **1994**, *27*, 892.

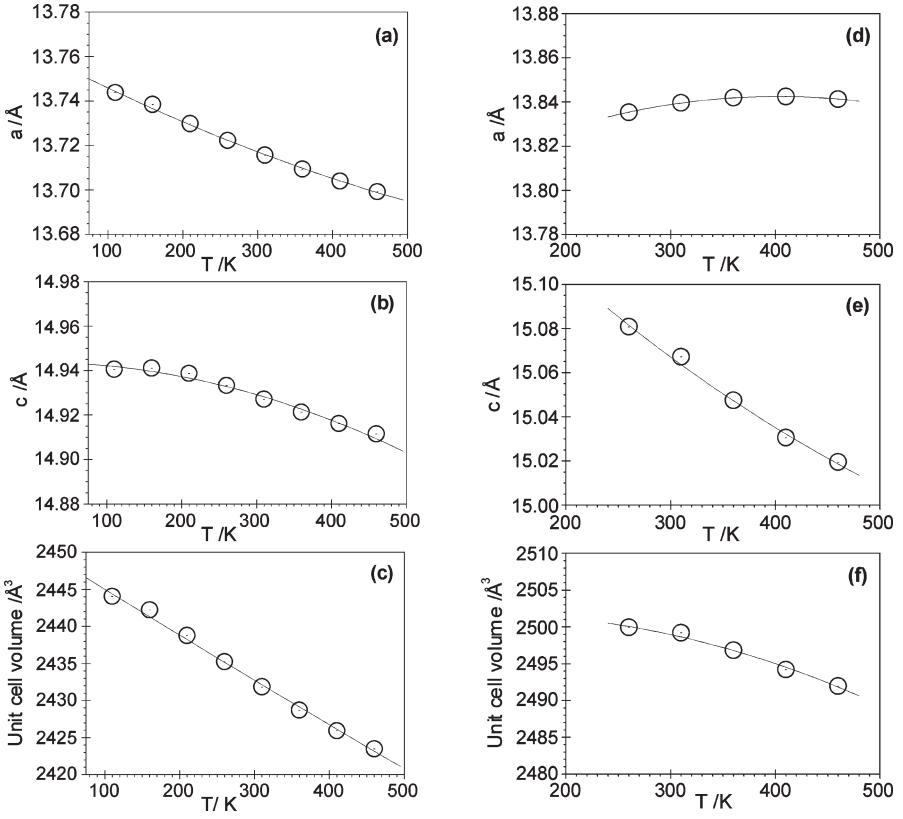

Figure 2. Plots of the variation of the cell parameters and volume with temperature for AlPO-34: (a) *a*, (b) *c*, and (c) volume; and for GaPO-34: (d) *a*, (e) *c*, and (f) volume. Note in these plots and those presented later, the error bars on the points are considerably smaller than the points themselves. The lines are fitted polynomials (see text).

dehydrated of AlPO-34.[38] A small amount ($< 0.1\%$ of the total diffracted intensity) of impurity was noticed in both samples but this gave only one peak that did not overlap with any peaks due the sample, hence a small region of the diffraction data was excluded from subsequent analysis. Upon our initial cooling of GaPO-34 to 110 K we observed an unexpected phase transition, and in fact, the data recorded at 160 and 210 K showed the presence of this low-temperature form along with the expected trigonal polymorph. The powder X-ray diffraction data of this new low temperature polymorph can be indexed using a monoclinic space group $C2/m$ (see the Supporting Information), and we intend to investigate its structure at a later date: for the purposes of the current work, we compare the thermal behavior of the trigonal polymorph with the isostructural AlPO-34 (which remains trigonal down to 110 K). In the case of AlPO-18, the unit cell was refined using the orthorhombic spacegroup *Cmcm*, consistent with the 298 K structure reported by Simmen et al. for the same material.[32] Figures 2 and 3 show plots of cell parameters vs temperature for the three materials, and Table 1 shows linear thermal expansivity coefficients calculated using standard expressions. Fits to thermal curves are given in the Supporting Information, and instantaneous values of volumetric thermal expansion coefficients thus calculated from the derivatives of fitted curves at room temperature, along with values previously reported for SiO_2 CHA in two separate studies, are shown in Table 1.

Both AlPO-34 and GaPO-34 (both CHA-type structures) show negative volume thermal expansion over the temperature ranges we have studied, with volume expansion coefficients of a magnitude comparable to other zeolite materials (although still less than the record holder AlPO-17 for which $\alpha_V = -35.1 \times 10^{-6}$ K^{-1} [17]) but also distinct anisotropy. The comparison with the isostructural SiO_2−CHA shows that AlPO-34 has rather similar thermal behavior to the SiO_2 sample studied by Martinez-Iñesta and Lobo,[29] both in terms of the magnitude of the volume thermal expansivity and the linear expansivities of each of the cell parameters (note that although SiO_2 CHA has a higher symmetry because the T sites are not distinguished as they are for the $AlPO_4$ analogue, the hexagonal unit cell has the same total content for each material, allowing direct comparison). The SiO_2 sample studied by Woodcock et al. gave a larger volume thermal expansivity but, more puzzling, a different anisotropy in the thermal expansion coefficients of the cell parameters (see Table 1).[28] Martinez-Iñesta and Lobo in fact noted that although their measured pair distribution function at room temperature showed good agreement with the Woodcock et al. model from Rietveld refinement, the model at higher temperature did not match their experimental data well. Whether the origin of this discrepancy is the nature of the actual sample studied or in one of the previous diffraction experiments is not known.

(38) Poulet, G.; Sautet, P.; Tuel, A. *J. Phys. Chem. B* **2002**, *106*, 8599.

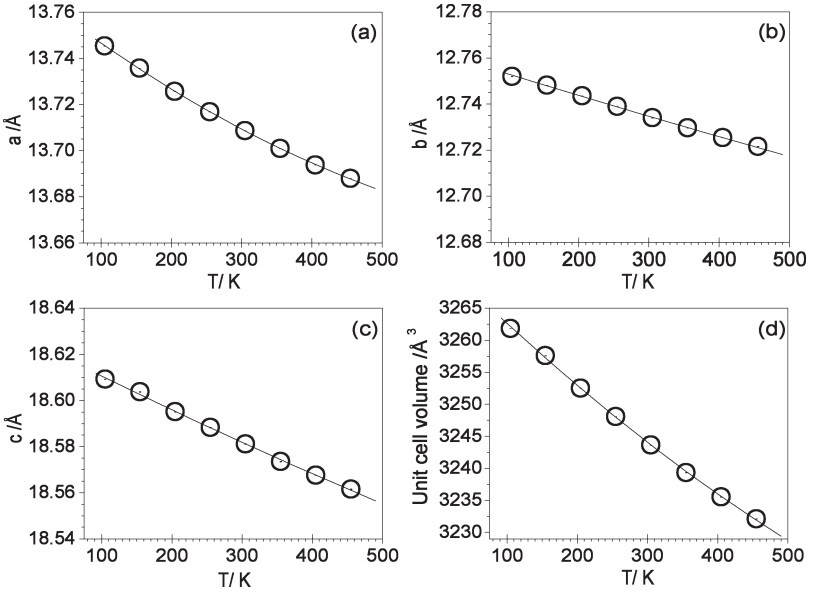

Figure 3. Plots of the variation of the cell parameters with temperature for AlPO-18: (a) *a*, (b) *b*, (c) *c*, and (d) volume, refined in orthorhombic spacegroup *Cmcm*.

Table 1. Thermal Expansion Behavior of the Materials Studied along with Previously Reported Values for CHA-Type SiO_2 from Two Published Studies

material	space group	temperature range (K)	α_a $(10^{-6}\,K^{-1})^a$	α_b $(10^{-6}\,K^{-1})^a$	α_c $(10^{-6}\,K^{-1})^a$	α_v $(10^{-6}\,K^{-1})^a$	α_v at 298 K $(10^{-6}\,K^{-1})^b$	ref
AlPO-34 (CHA)	$R\bar{3}$ (No. 148)	110−460	−9.27	−9.27	−5.54	−24.03	−24.77	this work
GaPO-34 (CHA)	$R\bar{3}$ (No. 148)	260−460	+2.15	+2.15	−20.30	−16.03	−12.25	this work
AlPO-18 (AEI)	*Cmcm* (No. 64)	105−455	−11.94	−6.81	−7.32	−26.01	−26.04	this work
SiO_2CHA	$R\bar{3}m$ (No. 166)	293−873	−8.24	−8.24	−13.30	−28.50	−28.62	Woodcock et al.[28]
SiO_2CHA	$R\bar{3}m$ (No. 166)	308−753	−9.11	−9.11	−3.08	−21.22	−21.22	Martinez-Iñesta and Lobo[c29]

[a] α_a, α_b, α_c, and α_V values are those obtained by linear fitting of the variation of cells parameters with temperature and calculated using the equation $\alpha_L = L - L_{ref}/L_{ref}(T - T_{ref})$. The reference temperature T_{ref} is the lowest temperature in the specified range. [b] The instantaneous values were calculated from the derivative of the polynomial fitted to the volume expansivity curve (see the Supporting Information). [c] Martinez-Iñesta and Lobo reported the cell parameters of the material at only two temperatures using the rhombohedral setting of the space group; we have recalculated the lattice parameters, and hence thermal expansion coefficients in the hexagonal setting to allow comparison with the other CHA-type materials.

Table 2. Published Thermal Expansion Behavior of SiO_2 Polymorphs and Phosphate Analogues

material	space group	temperature range (K)	α_a $(10^{-5}\,K^{-1})$	α_b $(10^{-5}\,K^{-1})$	α_c $(10^{-5}\,K^{-1})$	α_v $(10^{-5}\,K^{-1})$	ref
SiO_2(α−quartz)	$P3_121$ (No. 152)	298−838	+2.65	+2.65	+1.55	+6.95	39
$AlPO_4$(α−quartz-type)	$P3_121$ (No. 152)	298−841	+2.72	+2.72	+1.48	+7.01	40
$GaPO_4$(α−quartz-type)	$P3_121$ (No. 152)	306−1223	+1.84	+1.84	+0.71	+4.46	43
SiO_2(α−cristobalite)	P 4_12_12(No. 90)	301−503	+1.95	+1.95	+5.26	+9.30	41
$AlPO_4$(α−cristobalite)	$C222_1$(No. 20)	298−473	+2.74	+2.72	+4.45	+9.98	42
$GaPO_4$(α−cristobalite)	$C222_1$(No. 20)	298−873	+1.85	+1.98	+2.32	+6.22	42

Notwithstanding this, there is precedent to show that the isoelectronic SiO_2 and $AlPO_4$ polymorphs of a given structure type should have the same thermal behavior; indeed α-quartz and α-cristobalite forms of SiO_2 and $AlPO_4$ have similar thermal behaviors in both the magnitude and the anisotropy of the their thermal expansion coefficients, Table 2.[39−42] (To the best our knowledge there are no other reported results from an isoelectronic pair of low density zeolites analogues.) Therefore, the agreement between the thermal expansivity at room temperature of our sample of AlPO-34 CHA and the SiO_2 CHA studied by Martinez-Iñesta and Lobo is not unexpected.

In the case of GaPO-34, the volume thermal expansivity is also negative but has a magnitude of around 50% of that of its $AlPO_4$ and SiO_2 analogues. The thermal expansivity of GaPO-34 also shows a greater anisotropy with $\alpha_a = \alpha_b$ positive, whereas α_c is large and negative. This shows that despite an identical topology (see below) the GaPO-34 CHA-type material has a distinctly different thermal behavior to its AlPO-34 CHA-type analogue. To the best of our knowledge, there are no other reported studies on the thermal expansivity of $GaPO_4$ zeolite

(39) Kihara, K. *Eur. J. Mineral.* **1990**, *2*, 63.
(40) Muraoka, Y.; Kihara, K. *Phys. Chem. Miner.* **1997**, *24*, 243.
(41) Peacor, D. R. *Z. Kristallogr.* **1973**, *138*, 274.
(42) Achary, S. N.; Jayakumar, O. D.; Tyagi, A. K.; Kulshresththa, S. K. *J. Solid State Chem.* **2003**, *176*, 37.

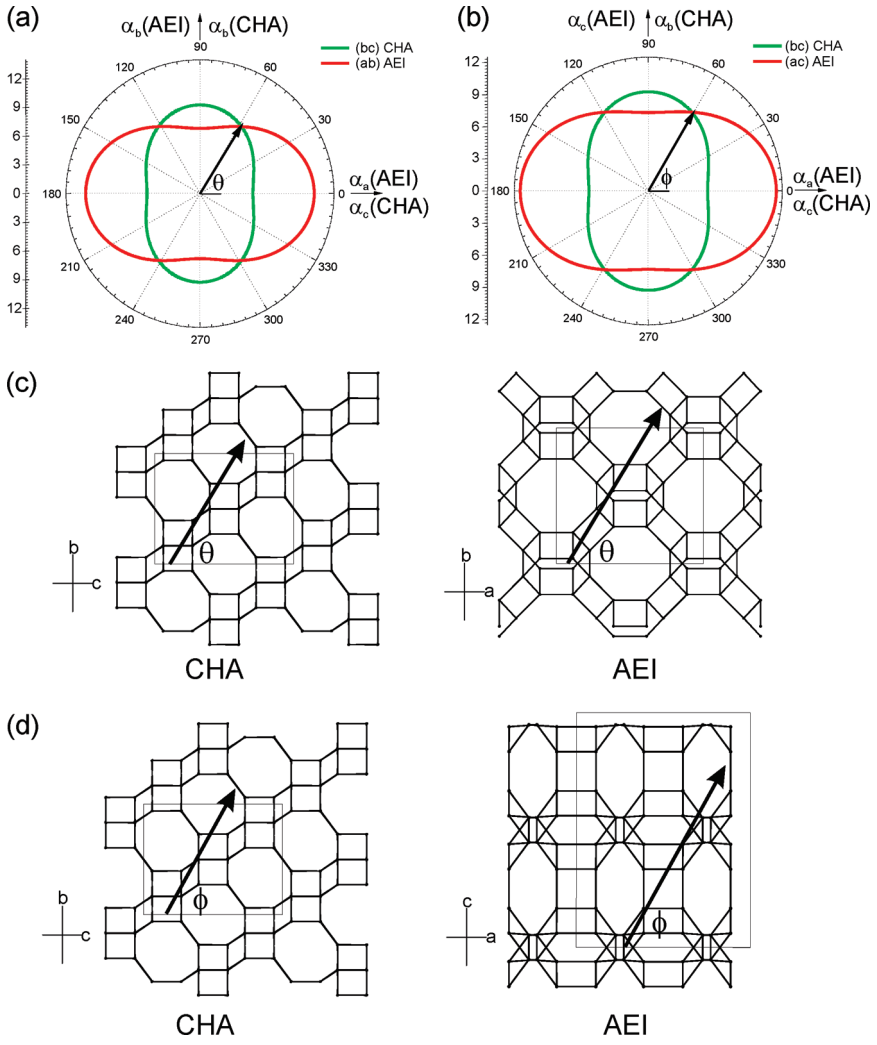

Figure 4. (a) Polar plots of axial thermal expansion coefficients for AlPO-34 CHA and AlPO-18 AEI in the *bc* and *ab* planes, respectively, and (b) the *bc* and *ac* planes, respectively, and (c, d) projections of the room temperature structures of the two materials in the same planes. In a and b, the scales represent the magnitude of the (negative) thermal expansion coefficient ($\times 10^{-6}$ K^{-1}). The arrows in c and d indicate directions that correspond to the directions of the intersections of the polar plots in a and b, as indicated by the angles θ and ϕ.

materials, but we do note that the $GaPO_4$ α-quartz and α-cristobalite materials have been reported to have smaller magnitudes of thermal expansion coefficients than their $AlPO_4$ or SiO_2 analogues, Table 2.[39−43] This suggests that replacement of aluminum by gallium in an extended phosphate can modify the thermal expansivity. This is consistent with recent work on $AlPO_4$−$GaPO_4$ solid solutions by Cambon et al., who showed that replacement of aluminum by gallium in the quartz-type structure reduces M−O−P angles and lessens their temperature dependence, possibly because of an enhanced covalent character of the bonds.[44]

To explore the relationship between the negative thermal expansion seen in AlPO-34 and AlPO-18, we have plotted polar plots of the axial thermal expansion coefficients in the *bc* plane of AlPO-34 using standard manipulation[45] and compared them with plots of the coefficients in the *ab* and *ac* planes of AlPO-18, panels a and b in Figure 4 (note that AlPO-34 is trigonal hexagonal, so such a simple comparison in other planes is not straightforward). Points of intersection within each of the plots correspond to the same magnitude of thermal expansivity in that direction (-8.23×10^{-6} and -8.40×10^{-6} K^{-1} at angles $\theta = 58.20°$ and $\phi = 61.10°$, respectively) and therefore might be related to some similarity in the structures of the two materials in these directions. To test this idea, panels c and d in Figure 4 show projections of the structures (the reference CHA-type and AEI-type structures taken from the IZA structure database[26]) viewed in the same planes as the polar plots with the directions of intersections of the polar plots marked: it can clearly then be seen that the direction of coincidence of the thermal expansivity maps onto a similarity of the structures in these directions. In both cases, the direction corresponds to a four-ring link between pairs of double six rings and an intersection of the "diameter" of an eight-ring opening. This strongly suggests that the long-range structural origin of thermal

(43) Haines, J.; Cambon, O.; Prudhomme, N.; Fraysse, G.; Keen, D. A.; Chapon, L. C.; Tucker, M. G. *Phys. Rev. B* **2006**, 73.
(44) Cambon, O.; Haines, J.; Cambon, M.; Keen, D. A.; Tucker, M. G.; Chapon, L.; Hansen, N. K.; Souhassou, M.; Porcher, F. *Chem. Mater.* **2009**, *21*, 237.
(45) Newnham, R. E., Properties of Materials, Anisotropy, Symmetry, Structure; Oxford University Press: Oxford, U.K., 2005.

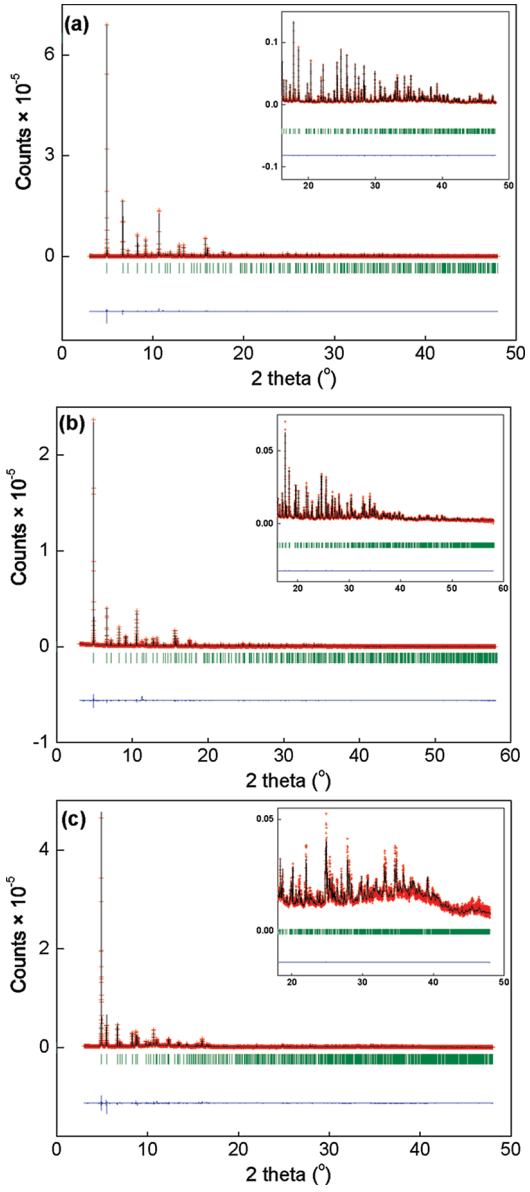

Figure 5. Final Rietveld fits of powder diffraction data at 300 K for (a) AlPO-34, (b) GaPO-34, and (c) AlPO-18. Points are experimental data, lines are the fitted model and the tick marks are allowed reflections of the appropriate spacegroup.

expansivity in these particular crystallographic directions is the same in each of materials and is dominated by particular structural responses to temperature that are common to both materials. This is perhaps not unexpected given the similarity in their structures, but this will be explored further below when we consider the atomic structure as a function of temperature.

3.2. Structural Response to Temperature. Rietveld refinement of atomic coordinates and thermal parameters at each temperature for the three materials was undertaken to understand the thermal behavior revealed by the variation of cell parameters with temperature. For AlPO-34 and GaPO-34 the room temperature structure of AlPO-34 published by Poulet et al.[38] was used as a starting point. (Note that a standard transformation of the rhombohedral setting of the published trigonal room temperature structure of AlPO-34 was converted to the hexagonal setting to provide a starting model that would allow later comparison with hexagonal SiO_2 CHA.) In the case of AlPO-18, although the room-temperature structure of Simmen et al. was best described using the monoclinic spacegroup $C2/c$ that distinguishes individual Al and P sites,[32] the symmetry was increased to orthorhombic *Cmcm* to reduce the number of parameters refined and to give satisfactory (physically reasonable) interatomic distances and angles. This means that aluminum and phosphorus atoms are no longer distinguished and are in fact modeled as an average tetrahedral (T) site, but a similar approach has been used previously for complex AlPO structures when analyzing similar powder diffraction data (such as the variable temperature X-ray diffraction study of AlPO-17[17]). To test the validity of this approach, we also refined the AlPO-34 structure as TO_2 in space-group $R\bar{3}m$ and indeed this gave the same behavior in T−T distances as Al−P distances in the first model. In the first stage of the refinement, the parameters of the peak shape profile were fixed from the values found during Le Bail extraction and the background was described as a set of points determined using linear interpolation. In the final cycle of least-squares refinements, scale factor, cell parameters, zero shift, thermal parameters, atomic positions, and peak shape parameters were refined. For AlPO-34 a free isotropic refinement strategy was used, and individual thermal parameters were defined for each atom with no restraints on atomic positions in the final refinement cycles. For AlPO-18 and GaPO-34, soft restraints on bond lengths and angles were used (T−O = 1.62 ± 0.02 Å for AlPO-18, and Ga−O = 1.81 ± 0.005 Å, P−O = 1.52 ± 0.005 Å for GaPO-34, and tetrahedral angles ±0.05° for GaPO-34 and ±0.03° for AlPO-18 from their starting values) and a global thermal parameter was refined. The full details of the Rietveld refinements, including resulting structures in CIF format, are given in the Supporting Information. Figure 5 shows the final fits for the three materials at room temperature.

The shortest interatomic distances and angles obtained for aluminum, gallium, and phosphorus atoms are concerned with chemical bonds to oxygen within tetrahedral primary building units, and these show little variation from ideal tetrahedral behavior as a function of temperature (see the Supporting Information). Although these are average, "apparent" distances, the data do show that to a first approximation we can consider the structures to be made up of rigid tetrahedral units, and that in order to explain their thermal expansivity, we must consider how larger structural units behave with temperature. Figures 6−8 show plots of intertetrahedral distances for AlPO-34, GaPO-34, and AlPO-18, respectively, defined as the shortest distance between T atoms with the structures. (Note that if the soft restraints on T−O distances were removed, the structure refinement gave the same trends in T−T distances (see the Supporting Information), despite physically unreasonable T−O distances, indicating that the T atom positions are well determined by our data analysis.) For AlPO-34, it can be seen that all

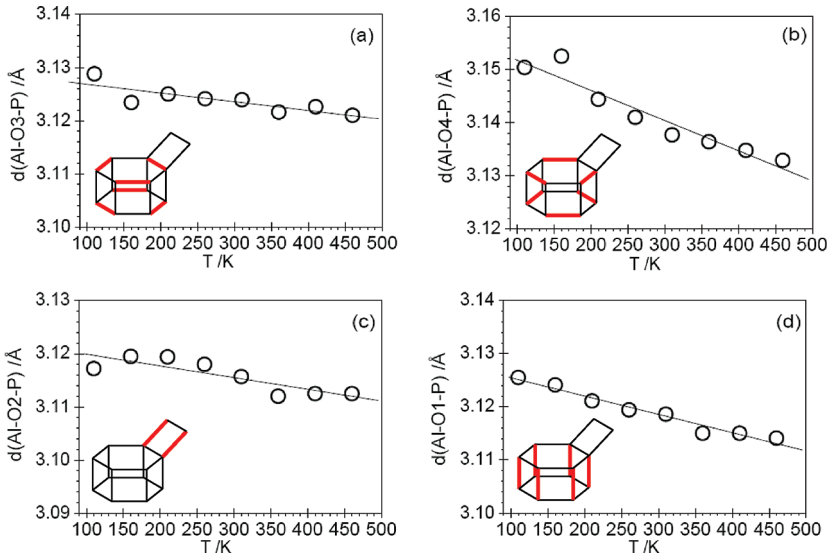

Figure 6. Plots of unique $T-T$ distances for AlPO-34 with temperature with their location indicated. Note that on the y-axis the linking oxygen between T sites is given but the distances are actually the $T-T$ distances.

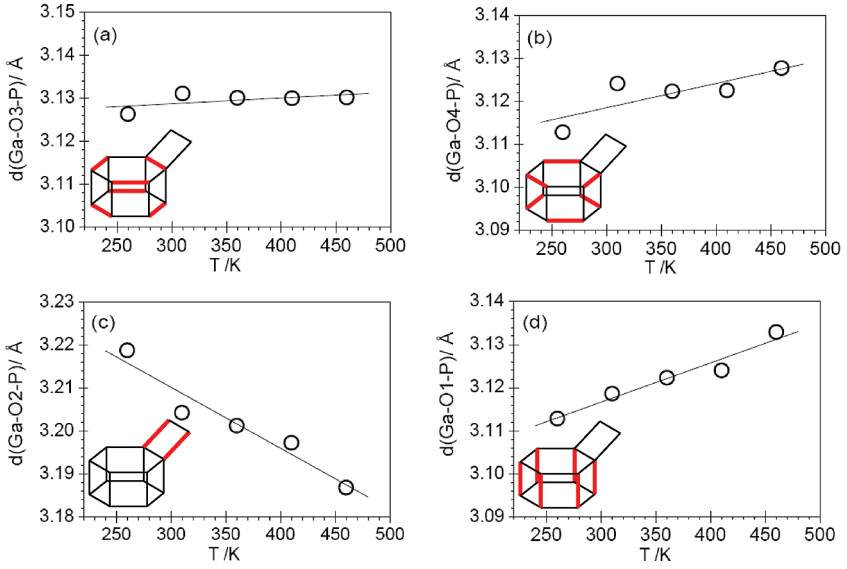

Figure 7. Plots of $T-T$ distances for GaPO-34 with temperature with their location indicated. Note that on the y-axis the linking oxygen between T sites is given but the distances are actually the $T-T$ distances.

Al−P distances show a clear contraction with temperature, although not by the same amount, Figure 6. In fact, certain bridging oxygen atoms appear to offer more flexibility than others. For AlPO-18, the situation is more complicated but there are clearly pairs of T atoms whose separation shortens with temperature (panels d and f in Figure 8). In the case of GaPO-34, only one unique Ga−P distance shortens with temperature (Figure 7c) and one Ga−P pair shows a distinct increase in distance with temperature (Figure 7d); this is consistent with the anisotropic behavior in thermal behavior of the unit-cell parameters. These observations are consistent with certain pairs of tetrahedral centers being pulled together by the transverse motion of a bridging oxygen as temperature increases, as has been used to explain the thermal behavior of related materials, such as AlPO-17 and siliceous FAU-type zeolite.[17,19]

In looking for some similarity between atomic displacement with temperature between each of the materials, the behavior of the double six-ring (D6R) secondary building unit provides a relationship. Figure 9 shows an idealized representation of the behavior of the double six rings as a function of temperature based on the data plotted in Figures 6−8, and which maintains the symmetry of crystal structures as indicated by the experimental data. For AlPO-34 and AlPO-18, the areas of the upper and lower six-ring faces of the D6R contract on increasing temperature due to expansion of half of the edges of each ring, the others expanding in alternating manner. In contrast, for GaPO-34, the area of the six-ring faces of the D6R both increase with increasing temperature, giving the positive α_a and α_b coefficients. It is not clear why the $GaPO_4$ material should behave differently than its $AlPO_4$ analogue from a structural point of view, although of course the local electron density of framework will differ

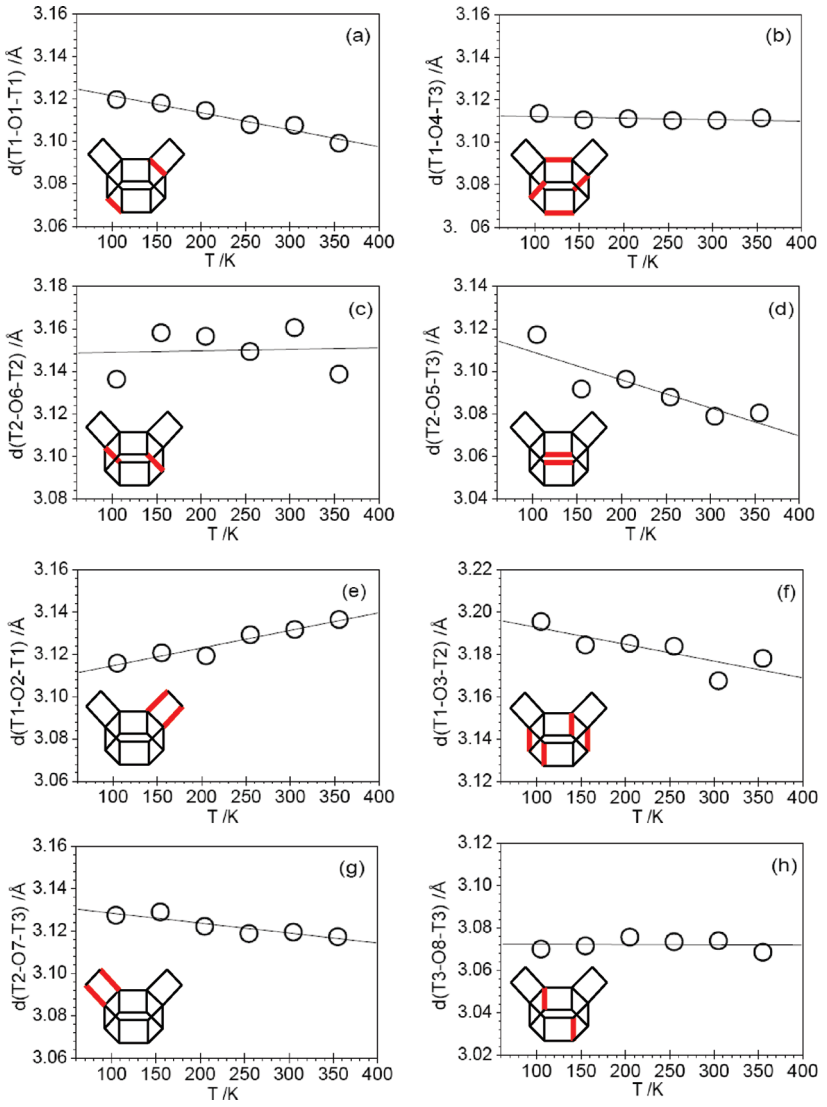

Figure 8. Plots of $T-T$ distances for AlPO-18 with temperature with their location indicated. Note that on the *y*-axis the linking oxygen between T sites is given but the distances are actually the $T-T$ distances.

between each. However, as noted above, it is established that the thermal properties of MPO_4 quartz materials depends on the nature of the metal M^{3+},[44] and indeed it is well-established that other properties of quartz homologues (such as piezoelectricity, density and dielectric constant anisotropy), depend on the M−O−P bond angle and hence the identity of M^{3+}.[46] It may be also observed that the chemistry of $GaPO_4$ zeotypes is known to differ from $AlPO_4$ analogues: for example, the instability of the gallium phosphates toward moist air (see Experimental Section) suggests an inherently different flexibility of the network that allows easy coordination of water, and our observation of a low-temperature phase transition to lower symmetry in GaPO-34 also indicates some different structural behavior. This is also backed by the work of Girard et al., who used computer simulation to analyze various gallophosphate forms of zeolites and noted that most gallium phosphates show instability upon template loss, unlike their aluminophosphate counterparts.[47]

Finally, it is useful to compare the behavior of the largest ring of tetrahedral atoms within the three materials, the eight ring. As shown in Figure 10, the eight ring shows a contraction with temperature across its largest dimension in each case. This is largest for the $GaPO_4$ material, and gives the large negative α_c value that then results in a net negative volume expansivity for GaPO-34. This fits with the view that low density regions of zeolite structure show the greatest flexibility and provides a common link between the three materials studied here. In their PDF analysis of CHA-type SiO_2, Martinez-Iñesta and Lobo also found that the eight-ring underwent contraction with temperature,[29] and in computational RUMs analysis of methanol sorption by chabazite Hammonds et al. found that the eight-ring channels possessed some considerable local flexibility, characterized by

(46) Philippot, E.; Palmier, D.; Pintard, M.; Goiffon, A. *J. Solid State Chem.* **1996**, *123*, 1.

(47) Girard, S.; Gale, J. D.; Mellot-Draznieks, C.; Férey, G. *J. Am. Chem. Soc.* **2002**, *124*, 1040.

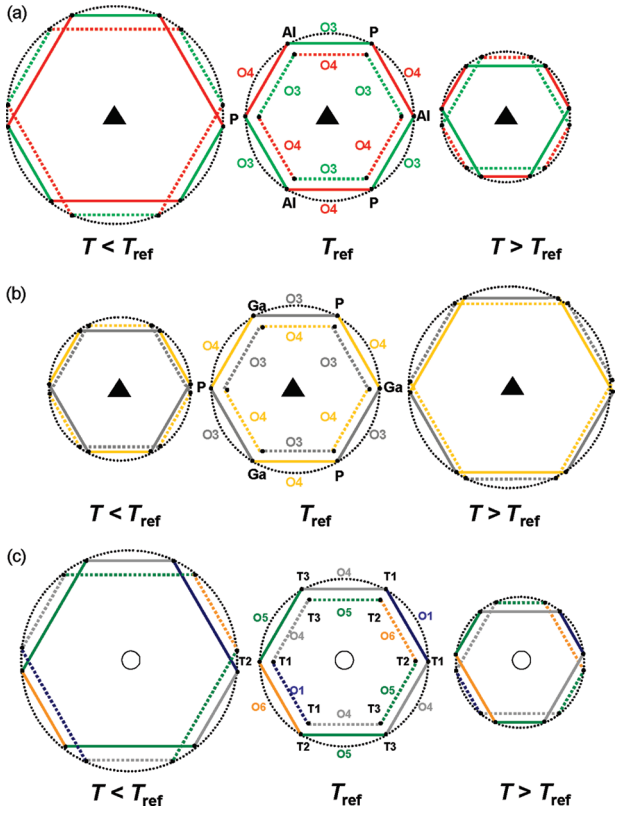

Figure 9. Idealized behavior of D6R secondary building units for (a) AlPO-34, (b) GaPO-34, and (c) AlPO-18 with temperature. The upper face of the D6R is represented by full line, and the lower face, dotted lines. Bridging oxygens are indicated with their site labels and certain symmetry elements of the appropriate space groups are indicated to show how symmetry is maintained upon structural distortion with temperature.

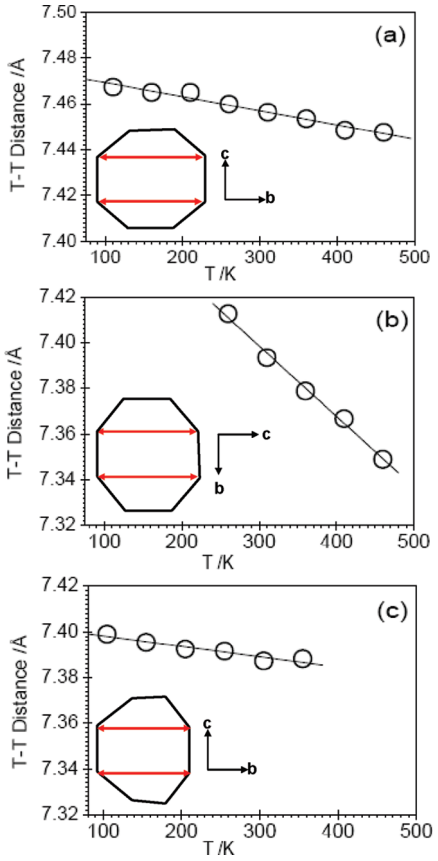

Figure 10. Behavior of the 8R with temperature for (a) AlPO-34, (b) GaPO-34, and (c) AlPO-18.

various floppy modes.[14] It is also important to the note that in our analysis of the behavior of the lattice parameters with temperature (vide supra), we noted that directions of similarity of the magnitude of the negative thermal expansion coefficients of AlPO-34 and AlPO-18 corresponded to a direction intersecting the diameter of the eight-rings; the full structural analysis bears out this conclusion.

Conclusions

A detailed powder X-ray diffraction study of three related phosphate zeotypes reveals negative thermal expansion in each, a result predicted by consideration of previous work on siliceous forms of one of the structures but until now not measured. The refined unit parameters for AlPO-34 and AlPO-18 as a function of temperature reveal that in certain crystallographic directions, the two materials possess negative thermal expansion coefficients of similar magnitudes, and these directions map onto parts of their crystal structures that show similar structural characteristics. A fuller analysis suggests that the two materials show the same structural distortion of double six-ring secondary building units with temperature and that the largest channel system, bounded by an eight ring, undergoes a distinct contraction with temperature. The behavior of GaPO-34 with temperature is rather different from its SiO_2 and $AlPO_4$ analogues, with a much more anisotropic expansivity, although the flexibility of the double six-ring secondary building unit and the eight-ring channels is a common key feature in defining the direction in which thermal contraction is seen. The results suggest that partial replacement of aluminum by gallium in phosphates would be a useful way in which to tune thermal expansion coefficients of these open-framework materials, although synthesis conditions would have be carefully tuned to allow isomorphous substitution: in the materials we have studied here, for example, the $GaPO_4$ and $AlPO_4$ analogues crystallize under rather different conditions using different organic structure directing agents. It should finally be noted that the use of Rietveld analysis gives models of average crystal structure with temperature, and the motion of flexible oxygen atoms is poorly defined. An analysis of the total scattering from these materials could provide more detailed atomic-scale models of the flexibility of the structures, as has been demonstrated for quartz polymorphs, for example.[48] This analysis, however, is presently a challenge for the more complex zeolites structures that generally have larger-volume unit cells and structures of lower symmetry than the dense SiO_2 polymorphs.

Acknowledgment. We thank EPSRC for funding this work (EP/C516591). We are grateful to Dr. Zoe Lethbridge (University of Warwick), Professor Ken Evans, Dr. Chris Smith, and Dr. Arnaud Marmier (University of Exeter) for

(48) Tucker, M. G.; Dove, M. T.; Keen, D. A. *J. Phys.-Condens. Matter* **2000**, *12*, L425.

useful discussions regarding various aspects of this work while in progress. The ESRF provided beamtime on ID31, and we thank Dr I. Margiolaki (ESRF) and Dr Franck Millange (Université de Versailles) for their assistance with running the experiments there. We also thank Dave Hammond, Department of Physics, University of Warwick, for measuring the TGA data.

Supporting Information Available: Thermogravimetric traces from all materials studied, Rietveld plot of low-temperature polymorph of GaPO-34, parameters of fitted polynomials of the thermal expansivity of the materials, final Rietveld parameters from the materials, and plots of T−O distances and angles (PDF). Full crystallographic data are provided in CIF format. This material is available free of charge via the Internet at http://pubs.acs.org/.